

Illuminant estimation using adaptive neuro-fuzzy interference system: supplemental document

This document will give some supplementary information, including ANFIS settings and an example of the membership functions, some visual results of our proposed method, and further discussions for the experimental results.

1. ANFIS MODELING

The structure of a typical ANFIS model with two inputs (x_1 and x_2) and one output (O^5) is demonstrated in Fig. S1, which consists of five layers defined as follows: Fuzzification layer, Multiplication layer, Normalization layer, Defuzzification layer, and Output layer [1].

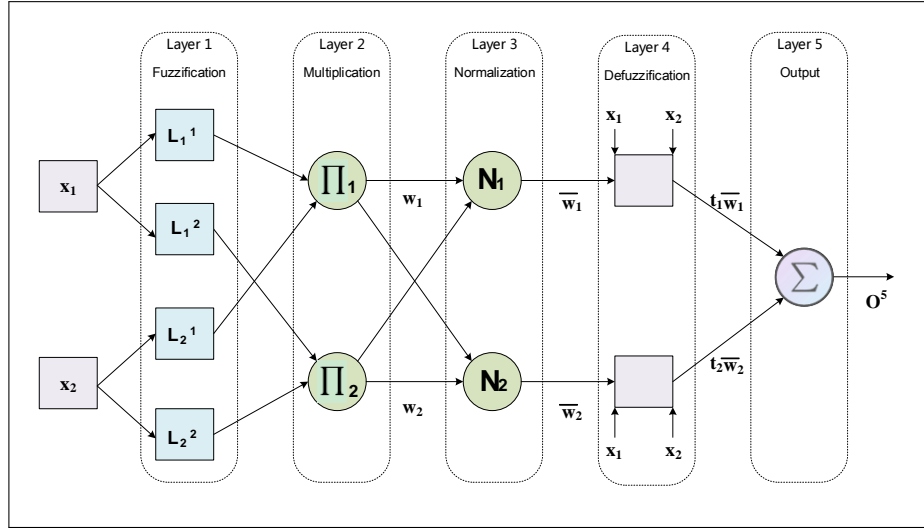


Fig. S1. ANFIS architecture example with two rules, two inputs (x_1 and x_2), and one output (O^5). L_1^1 and L_1^2 are the two linguistic labels for the first rule, and L_2^1 and L_2^2 are the two linguistic labels for the second rule [1].

Table S1 presents the specifications of the ANFIS models developed for predicting illuminant chromaticity components r , g , and b . Following these settings, we train each ANFIS model with the corresponding training samples (*IIFs*, *GTs*). After successful training, the parameters of each ANFIS model will be obtained, including the input membership functions. Fig. S2 shows an example for the input Gaussian membership functions used by the three developed ANFIS networks after the training procedure.

2. QUALITATIVE RESULTS

We provide some supplemental visual results for some typical scenes from Gehler-Shi and Cube+ datasets, as shown in Fig. S3 to S6. For each input image, we show the ground truth, our estimated illuminant color and resulting white-balanced image, and other estimated illuminant colors and resulting white-balanced images using the unitary algorithms (GW, GGW, WP, GE1, GE2, SOG, PCA-based, and LSR). In these figures, the color bar on the right side of images (a) and (b) shows the ground truth illuminant color. The color bar on the right side of images (c)-(k) shows the illuminant color estimated by the corresponding method, respectively. All images shown are rendered in sRGB color space.

Table S1. Specifications of the ANFIS models developed in this study.

Parameter	ANFIS settings
Initial FIS for training	genfis
Number of clusters	4
Output membership function	Linear
Number of outputs	1
Initial step size	0.01
Clustering type	Subtractive Clustering
Input membership function	Gaussian
Number of inputs	8~16
Training maximum epoch number	60

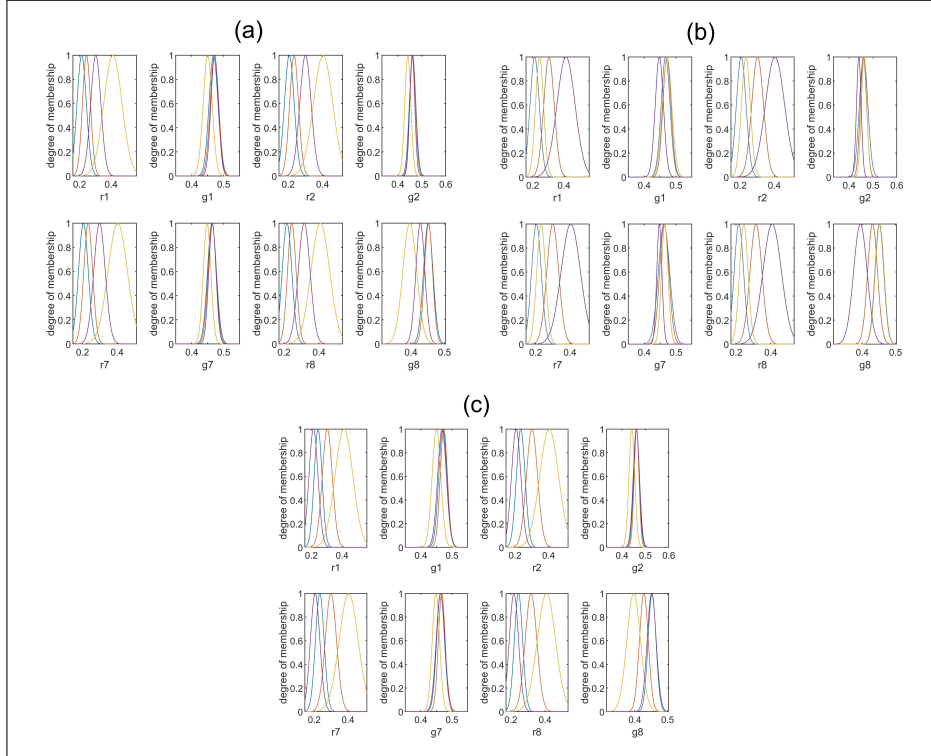


Fig. S2. Examples of membership functions used by the ANFIS models developed for (a) estimation of r component, (b) estimation of g component, and (c) estimation of b component. In these three models, the inputs are chromaticity values of r and g from the unitary algorithms: GW, WP, PCA-based, and LSR.

3. DISCUSSION AND FURTHER ANALYSIS

Different combination of unitary algorithms. By default, the proposed method uses the combination of eight unitary algorithms (GW, WP, SoG, GE1, GE2, GGW, PCA-based, and LSR), as we find for any image in our training dataset there are always some of these algorithms providing better illuminant estimation results. In Fig. S7, the histogram and cumsum plot give the distribution of the minimal AEs under these unitary algorithms for each image in Gehler-Shi and Cube+ dataset. It can be seen that for most images, 1950 out of 2275, there is a unitary algorithm to estimate illuminant color with AE being less than 3. With AE being less than 4, it is 2047 vs. 2275.

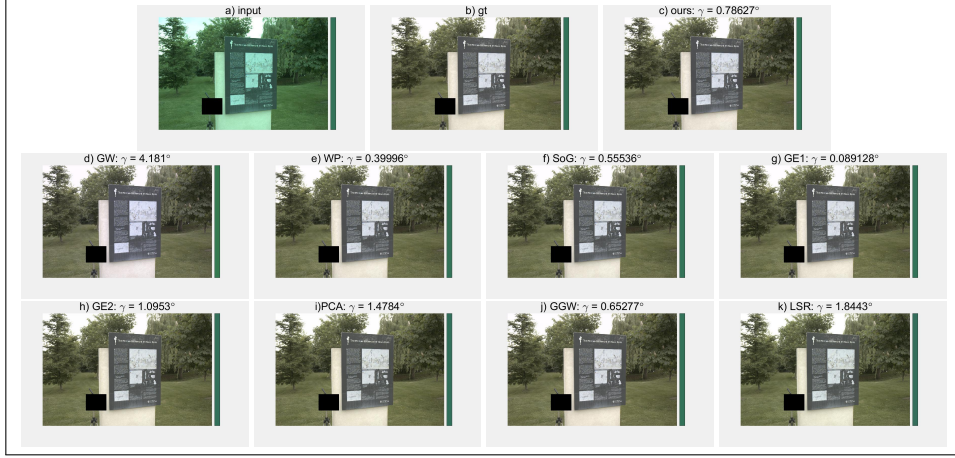


Fig. S3. Example results for natural lighting scene taken from the Gehler-Shi dataset: (a) input image; (b) ground truth (c) ours; (d)-(k) GW, GGW, WP, GE1, GE2, SOG, PCA-based, and LSR, respectively. All images shown are rendered in sRGB color space.

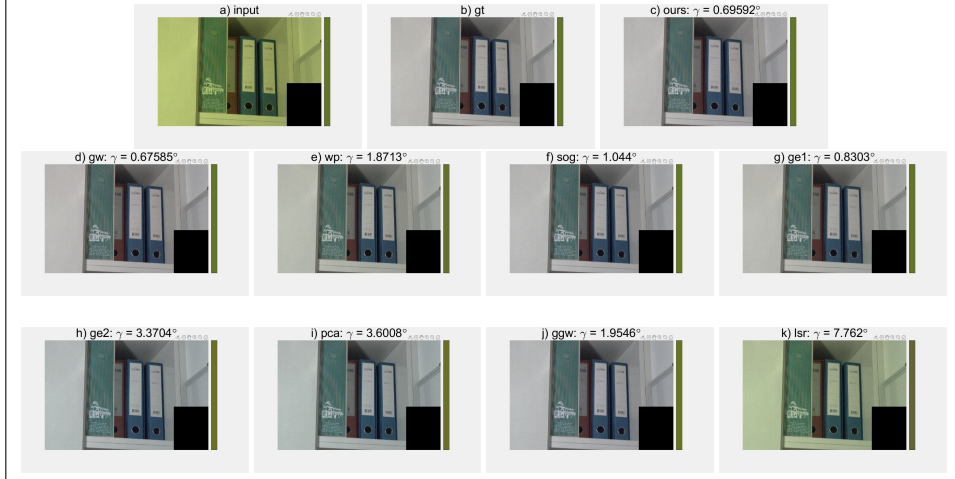


Fig. S4. Example results for indoor scene taken from the Cube+ dataset: (a) input image; (b) ground truth (c) ours; (d)-(k) GW, GGW, WP, GE1, GE2, SOG, PCA-based, and LSR, respectively. All images shown are rendered in sRGB color space.

This figure shows that if we use an appropriate, linear or nonlinear, combination of these unitary algorithms, it is possible to achieve better accuracy of illumination estimation. To further exploit better combination relationships, we design several combinations of these unitary algorithms to implement the proposed method. Some of them contain less than eight unitary algorithms. The experimental results are shown in Table S2. The results indicate that the configuration with the combination of GW, WP, PCA-based, and LSR results in the best illuminant estimation accuracy. It should be noted that this optimal combination might be just applicable for our experiments based on Gehler-Shi and Cube+ dataset. This experiment also indicates that seeking optimal combination is necessary to improve performances for illuminant estimation.

Using sparse weight matrix. In the proposed method, we use CDF weight vector η and IIF weight matrix ω to measure what degree an image belongs to each cluster. We can define an integrated weight matrix $W = [w_{ij}]$, $i = 1, 2, \dots, k_1$, $j = 1, 2, \dots, k_2$, where $w_{ij} = \eta_i \cdot \omega_{ij}$ is the final weight for the ij -th ANFIS predictor. Since commonly there are many elements in η and ω much less than 1 and very near to zero, i.e., the weights or possibilities for an image belonging to some clusters are very low, we can set all these elements' values to zero and then recalculate the values of other elements. For simplicity, we set a threshold ϵ for w_{ij} . If $w_{ij} < \epsilon$, set $w_{ij} = 0$. W will

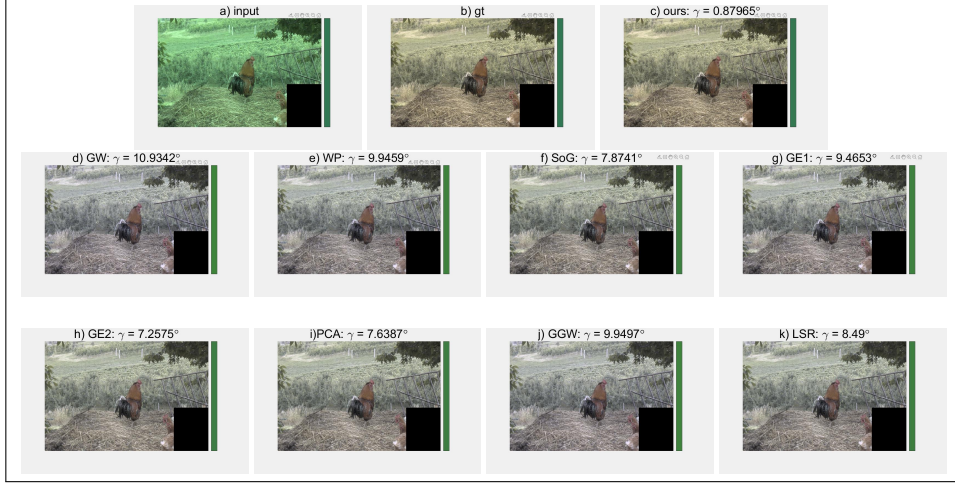


Fig. S5. Example results for outdoor natural lighting scene taken from the Cube+ dataset: (a) input image; (b) ground truth (c) ours; (d)-(k) GW, GGW, WP, GE1, GE2, SOG, PCA-based, and LSR, respectively. All images shown are rendered in sRGB color space.



Fig. S6. Example results for outdoor artificial lighting scene taken from the Cube+ dataset: (a) input image; (b) ground truth (c) ours; (d)-(k) GW, GGW, WP, GE1, GE2, SOG, PCA-based, and LSR, respectively. All images shown are rendered in sRGB color space.

become a sparse matrix \bar{W} . To assure the element summary of each row of \bar{W} to be 1, recalculate $w_{ij} \geq \varepsilon, i = 1, 2, \dots, k_1, j = 1, 2, \dots, k_2$ as below:

$$\bar{w}_{ij} = \frac{w_{ij}}{\sum w_{ij^*}}, \quad (S1)$$

where $\sum w_{ij^*}$ represents the summary of all elements greater than ε in the i -th row of W .

We conducted an experiment using the sparse weight matrix by setting ε between [0.01, 0.25]. We find the results change towards slightly improvement along with the increasing value of ε and the best performance corresponds to $\varepsilon = 0.25$, as Table S3 shows. By using the sparse weight matrix, we just need to weight a small number of outputs from ANFIS models, and the computation effort will reduce much more.

REFERENCES

1. M. Seyyedattar, M. M. Ghiasi, S. Zendehboudi, and S. Butt, "Determination of bubble point pressure and oil formation volume factor: Extra trees compared with LSSVM-CSA hybrid

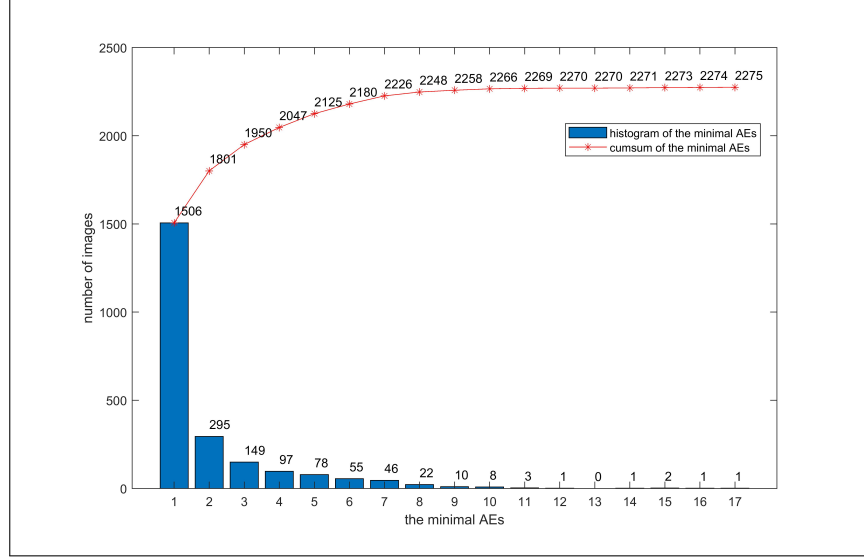


Fig. S7. Histogram and cumsum plot of minimal AEs. This figure shows the distribution of the minimal AEs for each image in the Gehler-Shi dataset or the Cube+ dataset using the eight unitary algorithms. It can be seen that for most images in the training dataset there is at least one unitary algorithm to estimate its illuminant color resulting in AE no more than 3.

Table S2. Statistical metrics on Gehler-Shi and Cube+ dataset using different combination of unitary algorithms (the lower, the better).

Combinations of unitary algorithms	Mean	Median	Trimean	Best 25%	Worst 25%
<i>GW, WP, SoG, GE1, GE2, GGW, PCA – based, LSR</i>	2.20	1.46	1.60	0.40	5.31
<i>GW, WP, SoG, GE1, GE2, GGW, PCA – based</i>	2.32	1.50	1.67	0.45	5.62
<i>GW, WP, SoG, GE1, GE2, GGW, LSR</i>	2.21	1.47	1.62	0.40	5.33
<i>GW, WP, SoG, GE1, GE2, GGW</i>	2.27	1.50	1.68	0.44	5.44
<i>GW, WP, SoG, GE1, PCA – based, LSR</i>	2.07	1.36	1.50	0.39	5.00
<i>GW, WP, SoG, GGW, PCA – based</i>	2.20	1.42	1.58	0.38	5.39
<i>GW, WP, SoG, GGW, LSR</i>	2.12	1.38	1.53	0.39	5.16
<i>GW, WP, SoG, GE1</i>	2.19	1.43	1.60	0.41	5.29
<i>GW, WP, GE2, GGW</i>	2.15	1.46	1.62	0.42	5.12
<i>Ours (GW, WP, PCA-based, LSR)</i>	1.96	1.28	1.42	0.36	4.77

Table S3. Statistical metrics on Gehler-Shi and Cube +dataset using sparse weight vector and matrix (the lower, the better).

Threshold setting	Mean	Median	Trimean	Best 25%	Worst 25%
0.01	2.17	1.47	1.65	0.44	5.08
0.05	2.14	1.43	1.61	0.41	5.04
0.1	2.08	1.37	1.56	0.38	4.97
0.15	2.03	1.34	1.51	0.37	4.85
0.2	1.99	1.32	1.48	0.36	4.78
0.25	1.97	1.30	1.46	0.36	4.77

and ANFIS models,” Fuel **269**, 1–18 (2020).